

Smooth interface effects on the Raman scattering in zinc-blende AlN/GaN superlattices

E. F. Bezerra, V. N. Freire, A. M. R. Teixeira, M. A. Araújo Silva, P. T. C. Freire, J. Mendes Filho, and V. Lemos*

Departamento de Física, Universidade Federal do Ceará, Centro de Ciências, Caixa Postal 6030, Campus do Pici, 60455-760 Fortaleza, Ceará, Brazil

(Received 27 October 1999)

Raman spectra of $(\text{AlN})_{8-\delta}/(\text{Al}_x\text{Ga}_{1-x}\text{N})_\delta/(\text{GaN})_{8-\delta}/(\text{Al}_x\text{Ga}_{1-x}\text{N})_\delta$ superlattices with interface thickness varying between $\delta=0$ and $\delta=3$ are calculated. The influence of the nonabrupt interface related broadening is described in the complete range of scattering, with special attention to the modes giving stronger contribution to the Raman intensity. It is shown that the dispersion of folded acoustic phonons does not change appreciably with the interface smoothing. For $\delta=0$ the Raman spectra display new peaks due to the enhancement of some confined optical modes.

I. INTRODUCTION

The AlN/GaN superlattice (SL) belongs to the III–V nitride family that is suited to the technology of a new generation of devices including laser diodes emitting in the blue to ultraviolet range.¹ Most experimental studies have been performed on the wurtzite parent nitride compounds.^{2–5} However, devices with a zinc-blende (ZB) structure would have considerable advantages. This is particularly true for GaN due to its higher saturated electron drift velocity, easy cleavage, and lower band energy,^{6–9} which is especially useful for laser diode applications.¹⁰ Also, the ZB nitrides are expected to have higher mobility, due to the decrease of the phonon number for the higher symmetry structure. Therefore, information on the vibrational spectroscopy of this new class of material is strongly desirable. The AlN/GaN SL dynamics calculations reported to date were restricted to the sharp (ideal) interface picture and used parameters derived from experimental data on the wurtzite bulk materials.^{11–13} The results indicate the existence of both propagating optical and confined acoustic modes due to the smaller anion mass, which is in striking contrast with the phonon behavior in GaAs/AlAs SL's.

Recently, experimental phonon scattering results from the ZB nitrides have become available.^{14,15} By the use of such data it is possible to obtain results that can be tracked back to experiments. In addition, the model, to be reliable, should include the interdiffusion of ions at the SL interfaces that can play a crucial role on the Raman scattering. This is suggested from several studies performed with isostructural GaAs/AlAs SL's, which demonstrated the need to consider smooth (non-abrupt) interfacing, either to reproduce folded acoustic phonon spectra¹⁶ or to have reasonable agreement between calculated and experimental optical phonon frequencies.^{17,18} In the case of wurtzite GaN/Al_xGa_{1-x}N SL's, experimental evidence for cation intermixing in narrow quantum wells (~ 2 nm) points to the graded alloy interface region being as wide as the well width itself, causing the GaN A₁(LO) phonon mode to broaden and shift 7 cm^{-1} to higher frequency.⁴ It is important to remark that the smooth interface width in the GaN/Al_xGa_{1-x}N SL's is much wider than the interfaces found in GaAs/AlAs SL's,¹⁸ indicating that the nitride-based SL's should be more sensitive to smooth interfacing. There-

fore, a description of the vibrations in AlN/GaN SL's has to consider the existence of nonideal (nonabrupt) interfaces to be realistic.

A study of smooth interfacing effects on the dispersion relations and Raman spectra of $(\text{AlN})_{8-\delta}/(\text{Al}_x\text{Ga}_{1-x}\text{N})_\delta/(\text{GaN})_{8-\delta}/(\text{Al}_x\text{Ga}_{1-x}\text{N})_\delta$ SL's is performed in this work, with the interface thickness δ varying in steps of one to three monolayers (ML). The folded acoustic phonons calculated using the linear chain model are shown to be negligibly affected except for relative intensity changes in the higher orders of folding that disappear for wider interfaces, while the confined optical modes are sensibly shifted by the smooth interfacing. As a consequence, frequency overlapping may occur, giving rise to new Raman peaks in the spectra which are calculated through the bond-polarizability model. Our results for $\delta=3$ are in complete agreement with the experimental observation of Behr *et al.*,⁴ in which the GaN(LO) line modifications in single quantum wells (QW's) are attributed to interface effects.

II. RESULTS AND DISCUSSION

Each atom in the linear chain model (LCM) represents a plane of atoms in the actual SL, and their associated phonons propagating along the [001] axis can be described through a one-dimensional set of equations of motion. Restricting interaction to nearest and next-nearest-neighbors forces, the equations of motion can be solved in the harmonic approximation, and their eigenvalues and eigenvectors are obtained by diagonalization of the dynamical matrix. The alloyed interface was considered in the virtual-crystal approximation, which is appropriate to describe one-mode-type behavior of longitudinal vibrations in *c*-Al_xGa_{1-x}N.¹⁴ Based on the fact that the macroscopic effects are produced by interface broadening while the alloying is known to play a less relevant role,^{12,19} the aluminum molar fraction in the interfacial monolayers was taken as $x=0.5$. The bond-polarizability model, which provides a good description of optical modes,²⁰ was used to calculate the Raman spectra of the AlN/GaN SL's. In the acoustic-phonon region, the principal scattering mechanism involves the photoelastic coupling. In general, experimental results have been well reproduced by including this effect in the elastic continuous model.^{21,22} On

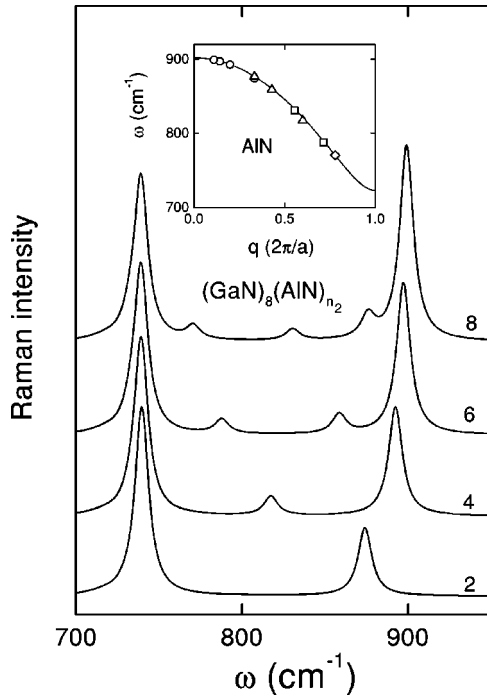


FIG. 1. Calculated Raman spectra for $(\text{GaN})_8/(\text{AlN})_{n_2}$, with $n_2 = 2, 4, 6, 8$, and ideal interfaces. The inset compares the bulk phonon dispersion and the mapping of the SL confined phonon frequencies. Different symbols were used to distinguish among the several confined indexes.

the other hand, several Raman studies in Ge/Si based SL used a modified bond-polarizability model to interpret their data.¹⁹ This later form was adopted in this work to provide for the scattering efficiency of the $(\text{AlN})_{8-\delta}/(\text{Al}_{0.5}\text{Ga}_{0.5}\text{N})_{\delta}/(\text{GaN})_{8-\delta}/(\text{Al}_{0.5}\text{Ga}_{0.5}\text{N})_{\delta}$ SL's. The polarizability constants were assumed to have fixed values throughout the SL. The dispersion for the sharp interface (ideal) $(\text{AlN})_{n_1}/(\text{GaN})_{n_2}$ SL, with $N = n_1 + n_2$, is formed by N optical and N acoustic branches.¹⁸ For $n_1 = n_2 = 8$, the SL is expected to have 16 optical and 16 acoustic phonon branches.

Within these assumptions, it was possible to retrieve the AlN bulk dispersion using the Raman scattering of confined optical phonons from $(\text{GaN})_{n_1}/(\text{AlN})_{n_2}$ SL's, and a mapping procedure. Calculated Raman spectra for ideal $(\text{GaN})_8/(\text{AlN})_{n_2}$ SL's ($n_2 = 2, 4, 6, 8$) are presented in Fig. 1, where the selected spectra are labeled with the corresponding n_2 numbers and the inset depicts the bulk AlN dispersion. The open symbols are the result of a mapping performed using the effective wave vector $q = m\pi/(n_2 + \lambda)a$, where m is the order index, a is the AlN monolayer thickness, and λ is a parameter describing the penetration of the wave function of AlN vibrations into the GaN layers. The value $\lambda = 1$ was found to produce a perfect mapping, as can be seen in the inset of Fig. 1. The bulk c -AlN and c -GaN mode frequencies (as used in the LCM model) and the force constants are listed in Table I. The zone edge phonon frequencies were obtained from calculations of the c -AlN (Ref. 23) and c -GaN (Ref. 24) dynamical properties. The c -AlN LO frequency is the value measured by Harima *et al.*,¹⁴ while that for c -GaN is an average among several experimental data.¹⁵ The fitted force

TABLE I. Bulk AlN and GaN mode frequencies as used in the mode to derive the force constants k , q_1 , and q_2 . The frequency values are in units of cm^{-1} .

	LA	LO (Γ)	LO (X)	k	q_1	q_2
AlN	594 ^a	902 ^b	723 ^a	222.83	30.02	-2.69
GaN	351 ^c	740 ^d	710 ^c	189.71	32.76	10.00

^aFrom Ref. 23.

^bFrom Ref. 14.

^cFrom Ref. 24.

^dAverage value taken from experimental data of Ref. 15.

constants differ appreciably from previous results,¹¹ probably due to an improved bulk dispersion related to the use of recently reported data. Comparison of the Raman spectra for the ideal interface SL's with those of Zi *et al.*¹¹ shows minor differences in the relative intensities but considerable changes in the peak positions.

The phonon dispersions for the $(\text{AlN})_{8-\delta}/(\text{Al}_{0.5}\text{Ga}_{0.5}\text{N})_{\delta}/(\text{GaN})_{8-\delta}/(\text{Al}_{0.5}\text{Ga}_{0.5}\text{N})_{\delta}$ SL's ($\delta = 1, 2, 3$) are presented in Fig. 2, where the dispersion of modes with origin in the bulk optical branches are depicted. The five lowest frequency modes are neither confined in the GaN nor in the AlN layer and their dispersions have a bulklike shape. They appear in the $[718, 738] \text{cm}^{-1}$ range and have extended nature due to the overlap of the bulk dispersion curves. Those modes should yield strong peaks in the Raman spectra as a consequence of the several quasidegenerated pairs at $q = 0$ in this range. However, the higher orders could preclude observation of some modes. In Fig. 2(a), the dispersion of

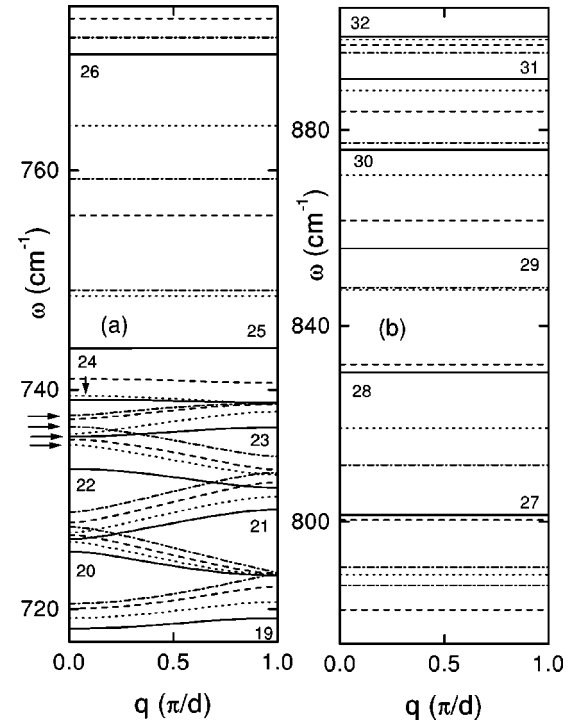


FIG. 2. Dispersion curves of (a) quasicontained modes and (b) AlN-confined modes for $(\text{AlN})_{8-\delta}/(\text{Al}_{0.5}\text{Ga}_{0.5}\text{N})_{\delta}/(\text{GaN})_{8-\delta}/(\text{Al}_{0.5}\text{Ga}_{0.5}\text{N})_{\delta}$ SL's, with: $\delta = 0$ (solid lines), $\delta = 1$ (dotted lines), $\delta = 2$ (dashed lines), and $\delta = 3$ (dot-dashed lines). The arrows point to the overlap of frequencies and the numbers specify the modes.

TABLE II. Confined optical phonon wave number, ω_0 , and the shifts δ_{i0} ($i=1,2,3$) observed by considering smooth interfacing of 1 ML, 2 ML, and 3 ML, respectively. All values are in units of cm^{-1} , and correspond to $q=0$.

	ω_0	δ_{10}	δ_{20}	δ_{30}
31	890.5	-2.5	-6.6	-13.1
30	875.9	-5.2	-14.4	-28.1
29	855.8	-8.4	-23.7	-44.3
28	830.6	-11.4	-30.3	-39.3
27	801.4	-12.2	-19.5	-14.5
26	770.6	-6.5	3.2	1.6
25	743.8	4.8	12.1	15.4
24	739.1	0.3	1.9	10.0

the five modes of lower frequency (numbered 19 to 23) are slightly modified when smooth interfacing is considered; the frequency shifts fall in the $[0.3, 3.8] \text{ cm}^{-1}$ range. The arrows label the frequency overlapping that occurs for some modes. The upper branches represent modes (24 to 26) that are strongly affected. Listed in Table II are only the corresponding shift values for the confined phonons that contribute significantly to the Raman spectrum and are drastically affected by the smooth interfacing. The existence of a $\delta=1$ interface does not affect appreciably the mode occurring at 739.1 cm^{-1} for $\delta=0$, but the broadening does (see Table II). The displacement picture shows this mode to be sharply confined (not shown here). Furthermore, it is expected to contribute strongly to the scattering for $\delta=0$, as would a truly confined GaN mode with $m=1$. For thicker interfaces it may contribute to the overlapping with neighboring frequency modes. The mode (25) at 743.8 cm^{-1} for $\delta=0$ is a quasicontained AlN mode, highly affected by the smooth interfacing. Its frequency is shifted upward by 15 cm^{-1} with interface broadening of 3 ML. Due to this important shift the mode is expected to resolve for thicker interfaces. The remaining mode (26) at 770.6 cm^{-1} for $\delta=0$ to be analyzed in Fig. 2(a) does not follow the usual trend of shifts being in a unique direction. Instead, it shifts downward for $\delta=1$ and upward for $\delta=2$ and $\delta=3$ (see Table II). Being confined in the AlN layer, its contribution to the Raman scattering should be noticeable.

The vibrations sharply confined to the AlN layers are depicted in Fig. 2(b). Their frequencies occur in the $[800, 900] \text{ cm}^{-1}$ range, where overlapping of the constituents bulk branches does not occur. The frequencies of folded acoustic phonons were observed to remain unaltered by the effect of smooth interfacing up to the 11th order of folding, except for some changes at the zone center and zone-edge gaps. The 12th folded phonon frequency is slightly modified by the interface broadening from $\delta=1$ to $\delta=3$. In the $[410, 580] \text{ cm}^{-1}$ range, the dispersion curves are flat revealing four modes that are sharply confined to the AlN layer. Their origin is the bulk AlN LA branch that extends far beyond the bulk GaN LA branch. The increasing of the interface thickness produces a systematic downshift of the frequencies. Despite the observed shifts amount up to -50.4 cm^{-1} , as higher order acoustic modes their contribution to the scattering should be negligible. Two almost degenerate modes (17,18) occurring in the $[710-715] \text{ cm}^{-1}$ range are quasicontained in

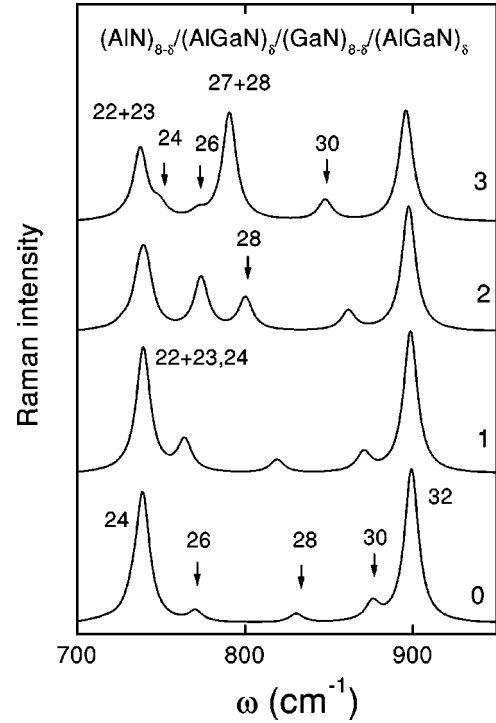


FIG. 3. Raman scattering from optic modes of $(\text{AlN})_{8-\delta}/(\text{Al}_{0.5}\text{Ga}_{0.5}\text{N})_{\delta}/(\text{GaN})_{8-\delta}/(\text{Al}_{0.5}\text{Ga}_{0.5}\text{N})_{\delta}$ SL's. The interface thickness δ which was considered in the calculations is indicated at the right side of each spectrum. The numbers close to the peaks indicate what are the modes whose contributions are the most important to their existence.

the GaN layer. Their frequencies are practically unaltered due to the interface smoothing.

Figure 3 shows the Raman spectra for the optical modes labeled according to the numbering given in Fig. 2. The dominant features in the lowest curve of Fig. 3 correspond to the GaN confined mode (at 739.1 cm^{-1} for $\delta=0$) and the truly confined AlN mode (at 899.1 cm^{-1} for $\delta=0$). The weak additional structures marked 26, 28, and 30, correspond to the AlN modes with index 7, 5, and 3, respectively. The effect of smooth interfacing in the $m=1$ AlN mode is just a small frequency shift. A similar, but more pronounced effect, is observed for the $m=3$ AlN mode. The remaining confined modes, however, are highly sensitive to the interface broadening, and remarkable intensity changes occur due to overlapping of almost degenerated modes. This should explain the strong peak appearing in Fig. 3 at 788 cm^{-1} for $\delta=3$. The overlapping is illustrated in Fig. 2(a) where two dotted-dashed lines around 788 cm^{-1} come as close as 3.8 cm^{-1} at $q=0$. With similar arguments one is able to identify the main contribution to the scattering and label the peaks in Fig. 3, accordingly. The calculated profile for $\delta=3$, in the GaN(LO) range, reproduces qualitatively the experimental results observed previously in narrow GaN/(AlGa)N QW's.¹⁹ The changes in line shape observed here are thus consistent with the interpretation given in Ref. 19 in terms of cation intermixing at the GaN/ $\text{Al}_x\text{Ga}_{1-x}\text{N}$ interfaces.

III. CONCLUSION

In conclusion, smooth interfacing effects on the Raman spectra of ZB $(\text{AlN})_{n_1}/(\text{GaN})_{n_2}$ SL's were studied using the

linear chain and bond-polarizability models. The approach extends existing results by considering interface broadening in describing the long-wavelength response. It was shown that for truly confined phonons the smooth interfacing effects are drastic. In the region of confined optic modes the spectra display new peaks due to the enhancement of modes activated by the smooth interfacing. On the other hand, it was shown that the confined acoustic modes do not contribute appreciably to the scattering. The dispersion of folded acoustic phonons remains unaltered, except for changes of the acoustic gaps. The main influence on those modes was the disappearance of higher order phonons for wider interfaces. Comparison of the overall smooth interfacing effects leads to the conclusion that optical modes are well suited as probe for interface broadening with both, frequencies and intensities,

highly affected. Reversing, it is possible to use the optical phonons Raman scattering as a reliable technique to characterize GaN/AlN SL's and determine ideal growth parameters.

ACKNOWLEDGMENTS

The authors would like to acknowledge the Conselho Nacional de Desenvolvimento Científico e Tecnológico (CNPq), the Fundação de Amparo à Pesquisa do Estado de São Paulo (FAPESP), and the Fundação de Amparo ao Ensino e Pesquisa da UNICAMP (FAEP) for financial support. One of us, V.L., thanks the Fundação de Amparo à Pesquisa do Estado do Ceará (FUNCAP), for financial support.

*Author to whom all correspondence should be addressed. Electronic address: volia@fisica.ufc.br, volia@ifi.unicamp.br. Permanent address: Instituto de Física Gleb Wataghin, Universidade Estadual de Campinas, Unicamp 13083-970 Campinas, São Paulo, Brazil.

¹S. Nakamura and G. Fasol, *The Blue Laser Diode* (Springer, Berlin, 1997); S. N. Mohammad and H. Morkoç, *Prog. Quantum Electron.* **20**, 361 (1996); I. Akasaki and H. Amano, *Jpn. J. Appl. Phys.* **36**, 5393 (1997), and references therein.

²R. Cingolani, G. Coli', R. Rinaldi, L. Calcagnile, H. Tang, A. Botchkarev, W. Kim, A. Salvador, and H. Morkoç, *Phys. Rev. B* **56**, 1491 (1997).

³M. Smith, J. Y. Lin, H. X. Jiang, A. Salvador, A. Botchkarev, W. Kim, and H. Morkoç, *Appl. Phys. Lett.* **69**, 2453 (1996).

⁴D. Behr, R. Niebuhr, J. Wagner, K.-H. Bachem, and U. Kaufmann, *Appl. Phys. Lett.* **70**, 363 (1997).

⁵M. F. MacMillan, R. P. Devaty, W. J. Choyke, M. Asif Khan, and J. N. Kuznia, *J. Appl. Phys.* **80**, 2372 (1996).

⁶J. Holst, L. Eckey, A. Hoffmann, I. Broser, B. Schöttker, D. J. As, D. Schikora, and K. Lischka, *Appl. Phys. Lett.* **72**, 1439 (1998), and references therein.

⁷K. H. Ploog, O. Brandt, H. Yang, and T. Trampert, *Thin Solid Films* **306**, 231 (1997), and references therein.

⁸S. Strite and H. Morkoç, *J. Vac. Sci. Technol. B* **10**, 1237 (1992).

⁹G. Ramírez-Flores, H. Navarro-Contreras, and A. Lastras-Martínez, *Phys. Rev. B* **50**, 8433 (1994).

¹⁰See Refs. 1–8 in X. L. Sun, H. Yang, L. X. Zeng, D. P. Xu, J. B. Li, Y. T. Wang, G. H. Li, and Z. G. Wang, *Appl. Phys. Lett.* **74**, 2827 (1999).

¹¹J. Zi, G. Wei, K. Zhang, and X. Xie, *J. Phys.: Condens. Matter* **8**, 6329 (1996).

¹²H. Grille and F. Bechstedt, *J. Raman Spectrosc.* **27**, 201 (1996).

¹³G. Wei, J. Zi, K. Zhang, and X. Xie, *J. Appl. Phys.* **82**, 622 (1997).

¹⁴H. Harima, T. Inoue, S. Nakahima, O. Okumura, T. Ishida, S. Yoshida, T. Koizumi, H. Grille, and F. Bechstedt, *Appl. Phys. Lett.* **74**, 191 (1999).

¹⁵H. Siegle, L. Eckey, A. Hoffmann, C. Thonsen, B. Meyer, D. Schikora, H. Hanken, and K. Lischka, *Solid State Commun.* **96**, 943 (1995); M. Giehler, M. Ramstainer, O. Brandt, H. Yang, and K. H. Ploog, *Appl. Phys. Lett.* **67**, 733 (1995). A. Tabata, A. P. Lima, J. R. Leite, V. Lemos, D. Schikora, B. Schöttker, U. Köhler, D. As, and K. Lischka, *Semicond. Sci. Technol.* **14**, 1 (1999); A. Tabata, A. P. Lima, L. K. Teles, L. M. R. Scolfaro, J. R. Leite, V. Lemos, B. Schöttker, T. Frey, D. Schikora, and K. Lischka, *Appl. Phys. Lett.* **74**, 362 (1999); A. Tabata, J. R. Leite, A. P. Lima, E. Silveira, V. Lemos, T. Frey, B. Schöttker, D. Schikora, and K. Lischka, *ibid.* **75**, 1095 (1999).

¹⁶V. I. Belitsky, T. Ruf, J. Spitzer, and M. Cardona, *Phys. Rev. B* **49**, 8263 (1994); T. Ruf, J. Spitzer, V. F. Sapega, V. I. Belitsky, M. Cardona, and K. Ploog, *ibid.* **50**, 1792 (1994); T. Ruf, V. F. Sapega, and M. Cardona, *J. Raman Spectrosc.* **27**, 271 (1996).

¹⁷K. T. Tsen, *J. Raman Spectrosc.* **27**, 277 (1996); K. T. Tsen, D. J. Smith, S. C. Y. Tsen, N. S. Kumar, and H. Morkoç, *J. Appl. Phys.* **70**, 418 (1991).

¹⁸B. Samson, T. Dumelow, A. A. Hamilton, T. J. Parker, S. R. P. Smith, D. R. Tilley, C. T. Foxon, D. Hilton, and K. J. Moore, *Phys. Rev. B* **46**, 2375 (1992).

¹⁹M. A. Araújo Silva, E. Ribeiro, P. A. Schulz, F. Cerdeira, and J. C. Bean, *Phys. Rev. B* **53**, 15 871 (1996); M. W. C. Dharma-Wardana, G. C. Aers, D. J. Lockwood, and J.-M. Baribeau, *ibid.* **41**, 5319 (1990).

²⁰B. Jusserand and M. Cardona, in *Light Scattering in Solids V*, edited by M. Cardona and G. Güntherodt, Topics in Applied Physics Vol. 66 (Springer, Heidelberg, 1989), p. 49.

²¹O. Pilla, V. Lemos, and M. Montagna, *Phys. Rev. B* **50**, 11 845 (1994); V. Lemos, O. Pilla, M. Montagna, and C. F. de Souza, *Superlattices Microstruct.* **17**, 51 (1995); V. Lemos, O. Pilla, and M. Montagna, *J. Raman Spectrosc.* **30**, 379 (1999).

²²X. Liu, D. Huang, Z. Jiang, and X. Wang, *Phys. Rev. B* **53**, 4699 (1996).

²³K. Karch and F. Bechstedt, *Phys. Rev. B* **56**, 7404 (1997).

²⁴K. Karch, J.-M. Wagner, and F. Bechstedt, *Phys. Rev. B* **57**, 7043 (1998).